



# A model study of the seasonal and long-term North Atlantic surface $p\text{CO}_2$ variability

J. F. Tjiputra<sup>1,6</sup>, A. Olsen<sup>2,5,6</sup>, K. Assmann<sup>3</sup>, B. Pfeil<sup>1,4,6</sup>, and C. Heinze<sup>1,5,6</sup>

<sup>1</sup>University of Bergen, Geophysical Institute, Bergen, Norway

<sup>2</sup>Institute of Marine Research, Bergen, Norway

<sup>3</sup>British Antarctic Survey, Cambridge, UK

<sup>4</sup>World Data Center for Marine Environmental Sciences, Bremen, Germany

<sup>5</sup>Uni Bjerknnes Centre, Uni Research, Bergen, Norway

<sup>6</sup>Bjerknnes Centre for Climate Research, Bergen, Norway

Correspondence to: J. F. Tjiputra (jerry.tjiputra@bjerknnes.uib.no)

Received: 30 September 2011 – Published in Biogeosciences Discuss.: 20 October 2011

Revised: 10 February 2012 – Accepted: 17 February 2012 – Published: 5 March 2012

**Abstract.** A coupled biogeochemical-physical ocean model is used to study the seasonal and long-term variations of surface  $p\text{CO}_2$  in the North Atlantic Ocean. The model agrees well with recent underway  $p\text{CO}_2$  observations from the Surface Ocean  $\text{CO}_2$  Atlas (SOCAT) in various locations in the North Atlantic. Some of the distinct seasonal cycles observed in different parts of the North Atlantic are well reproduced by the model. In most regions except the subpolar domain, recent observed trends in  $p\text{CO}_2$  and air–sea carbon fluxes are also simulated by the model. Over the longer period between 1960–2008, the primary mode of surface  $p\text{CO}_2$  variability is dominated by the increasing trend associated with the invasion of anthropogenic  $\text{CO}_2$  into the ocean. We show that the spatial variability of this dominant increasing trend, to first order, can be explained by the surface ocean circulation and air–sea heat flux patterns. Regions with large surface mass transport and negative air–sea heat flux have the tendency to maintain lower surface  $p\text{CO}_2$ . Regions of surface convergence and mean positive air–sea heat flux such as the subtropical gyre and the western subpolar gyre have a higher long-term surface  $p\text{CO}_2$  mean. The North Atlantic Oscillation (NAO) plays a major role in controlling the variability occurring at interannual to decadal time scales. The NAO predominantly influences surface  $p\text{CO}_2$  in the North Atlantic by changing the physical properties of the North Atlantic water masses, particularly by perturbing the temperature and dissolved inorganic carbon in the surface ocean. We

show that present underway sea surface  $p\text{CO}_2$  observations are valuable for both calibrating the model, as well as for improving our understanding of the regionally heterogeneous variability of surface  $p\text{CO}_2$ . In addition, they can be important for detecting any long term change in the regional carbon cycle due to ongoing climate change.

## 1 Introduction

Future climate change will largely depend on the evolution of the atmospheric  $\text{CO}_2$  concentration, which has been perturbed considerably by human activity during the past centuries. Studies have confirmed that less than half of the total anthropogenic  $\text{CO}_2$  emitted over the anthropocene era due to burning of fossil fuels, land use change, and cement production remains in the atmosphere today (e.g., Canadell et al., 2007; Le Quéré et al., 2009). The rest has been taken up by the terrestrial and ocean reservoirs mainly through plant photosynthesis and dissolution into seawater, respectively. The anthropogenic carbon uptake rate, however, is inhomogeneous in time and space and depends strongly on other external forcings acting on different spatial and temporal scales. In the ocean, the carbon uptake is influenced by processes ranging from short-term biological activity to long-term climate variability.

The North Atlantic ocean is an important region for ocean carbon uptake. Takahashi et al. (2009) show that the most intense  $\text{CO}_2$  sink area of the world oceans is located in the North Atlantic (for reference year 2000). For the year 2000, a modeling study by Tjiputra et al. (2010b) estimates a mean carbon uptake of  $21.6 \text{ g C m}^{-2} \text{ yr}^{-1}$  in the North Atlantic region between  $18^\circ\text{N}$  and  $66^\circ\text{N}$ . Of this amount, approximately half represents anthropogenic carbon. Because of this many studies, both observational and modeling, in the past decade have been dedicated to better understand the variability of air–sea  $\text{CO}_2$  fluxes in this region (e.g., Lefèvre et al., 2004; Lüger et al., 2006; Corbière et al., 2007; Thomas et al., 2008; Ullman et al., 2009; Watson et al., 2009; Levine et al., 2011; McKinley et al., 2011). In addition to altering the physical properties such as the temperature and ocean circulation of the North Atlantic, climate change will also feedback onto the biogeochemical processes by influencing the surface carbon chemistry and biological processes, crucial for oceanic carbon uptake. Therefore, understanding the role of present climate variability in controlling the North Atlantic carbon uptake remains a fundamental challenge and a necessary step in order to reduce the uncertainty associated with future climate projections.

On a time scale of less than one year, the air–sea  $\text{CO}_2$  fluxes in the North Atlantic are controlled by the seasonal variability of biological processes, temperature, wind speeds, and mixed layer depth (e.g., Lefèvre et al., 2004; Olsen et al., 2008; Bennington et al., 2009). On interannual and decadal timescales, long–term changes in the physical parameters associated with ocean circulation and climate variability dominate. The leading mode of climate variability in the North Atlantic is the North Atlantic Oscillation (NAO) (Hurrell and Deser, 2009). In this study, we assess the seasonal variability of the sea surface  $\text{CO}_2$  partial pressure ( $p\text{CO}_2$ ) simulated by an ocean biogeochemical general circulation model (OBGCM) as compared to available observations. Next, we apply a principal component statistical analysis to identify the primary and secondary mode of the surface  $p\text{CO}_2$  variability over the North Atlantic basin between 1960 and 2008. While the study by Thomas et al. (2008) has assessed the oceanic carbon uptake variability associated with the NAO, our study applies a different technique and covers a longer period in time.

Since the  $p\text{CO}_2$  is one of the carbon parameters that is directly measurable and represents the thermodynamical driver of air–sea  $\text{CO}_2$  exchange, we focus on this parameter for the comparison between model results and observations. Furthermore, with the advancement of measurement techniques over the last years, autonomous  $p\text{CO}_2$  measurement systems have been installed onboard many voluntary observing ships (VOS) to monitor the seawater  $p\text{CO}_2$  (Pierrot et al., 2009). Resulting from this is a substantial increase in the number of ship-based surface  $p\text{CO}_2$  measurements with relatively high coverage both in space and time (Watson et al., 2009). In certain regions, the amount of data has increased to the point

where month-to-month  $p\text{CO}_2$  and flux maps can be compiled. This allows for further insight into understanding the spatial and temporal variations of carbon dynamics in the North Atlantic region.

Another motivation for this study is to evaluate whether or not the governing processes behind the ocean carbon cycle model used in this study are sufficient to simulate the observed spatial and temporal  $p\text{CO}_2$  variability in the North Atlantic. Basin-wide characteristics of key ocean carbon cycle variability will be studied. This is an essential step because the model will be integrated into an Earth system model framework (e.g., Tjiputra et al., 2010a) and used to project future variability related to the climate change. Full assessment of the model, thus, will reduce the uncertainties and provide more confidence in future projections of the climate system and its associated carbon cycle feedback. It also serves as a prerequisite to test whether the model provides an appropriate first guess for use in advanced data assimilation schemes for more detailed global and regional now-casts and predictions and optimisation of governing parameters of the carbon cycle.

The paper is organized as follows: in the next two sections we describe the observations and model used in this study. Section four discusses the results of the analyses, and the study is summarized in section five.

## 2 Observations

In order to evaluate the model simulation, two independent data sets are employed. The first is from the CARINA (CARbon dioxide IN the Atlantic Ocean) data synthesis project which can be downloaded from <http://cdiac.ornl.gov/oceans/CARINA/> (Velo et al., 2009; Key et al., 2010; Pierrot et al., 2010; Tanhua et al., 2010). It is comprised of quality-controlled observations from 188 cruises focusing on carbon-related parameters. For the model comparison, we extracted the surface measurements of temperature (SST), salinity (SSS), dissolved inorganic carbon (DIC), and alkalinity (ALK) over the North Atlantic domain between 1990 and 2006. The data is then averaged and binned into monthly fields with  $1^\circ$  by  $1^\circ$  horizontal resolution.

The second data set consists of observations of surface  $f\text{CO}_2$  (i.e., fugacity of  $\text{CO}_2$ ) extracted from the Surface Ocean  $\text{CO}_2$  Atlas (SOCAT, Pfeil et al., 2012). SOCAT is the latest and most comprehensive surface ocean  $f\text{CO}_2$  data base, containing 6.3 million  $f\text{CO}_2$  values from 1851 voyages carried out between 1968 and 2007. SOCAT contains only measured  $f\text{CO}_2$  data (i.e., not calculated from, for example, dissolved inorganic carbon and total alkalinity data). The data have been predominantly analyzed through infrared analysis of a sample of air in equilibration with a continuous stream of seawater (Pierrot et al., 2009), but some of the older data were measured using an automated gas chromatographic system (Weiss, 1981). The SOCAT data have an accuracy of 4–5 ppm.

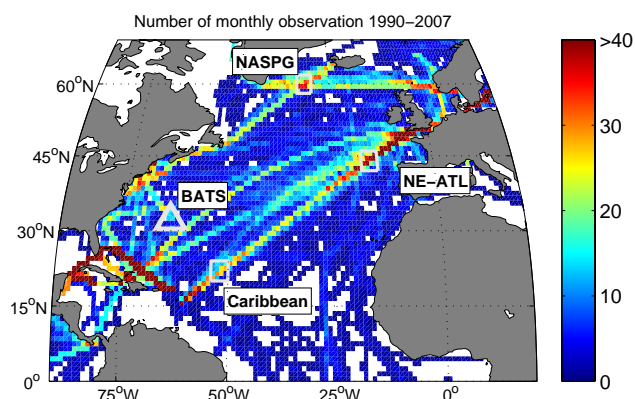


**Fig. 1.** Map of the total number of monthly underway observations of surface ocean  $p\text{CO}_2$  from the SOCAT database binned into one degree boxes. The value (out of a potential 216 monthly observations) is computed based on whether or not any observations are present for each month between 1990 to 2007.

In this study, we focus on the data sub-set from the North Atlantic. Figure 1 shows the spatial distribution of the data. Since the data is mainly used for comparison with the model in the seasonal time scale, we have selected three  $4^\circ$  by  $4^\circ$  regions based on the following criteria: (i) that they have good seasonal coverage (i.e., data from at least 8 out of 12 months) for at least three consecutive years and (ii) that they represented different oceanographic provinces (i.e., in those cases where several neighbouring  $4^\circ$  by  $4^\circ$  regions had the required seasonal coverage, we chose one). In addition, we also avoid regions close to the continental margins where the model does not perform adequately due to its fairly coarse resolution. Based on these criteria, we found three regions that fulfill the above conditions, as shown by the white rectangle in Fig. 1. To standardize the analysis, we use all data from these three locations spanning the period from 2002 to 2007 for comparison with the model simulation.

The first region, centered at  $60^\circ\text{N}$   $32^\circ\text{W}$ , is located in the subpolar gyre (NASPG) and was mainly covered by the routes of MV Skogafoss (processed by the United States, [http://www.aoml.noaa.gov/ocd/gcc/skogafoss\\_introduction.php](http://www.aoml.noaa.gov/ocd/gcc/skogafoss_introduction.php)) and MV Nuka Arctica of the Danish Royal Arctic Lines (Olsen et al., 2008). At this location, there is no data available for the year 2002, and only three months (June, November and December) for the year 2003. The second region is located in the northeast North Atlantic and was covered by the several VOS lines operated by Germany (Steinhoff, 2010), France, Spain (González Dávila et al., 2005; Padin et al., 2010), the UK (Schuster and Watson, 2007) and the United States, and is centered at  $44^\circ\text{N}$   $17^\circ\text{W}$  (NE-ATL). The last location is close to the Caribbean and is covered by routes of research vessels from Germany, United States, Spain, and the UK, centered at  $22^\circ\text{N}$   $52^\circ\text{W}$  (Caribbean). The three sub-domains represent different types of oceanic provinces from high- to low-latitudes.

In addition to the underway observations, the  $p\text{CO}_2$  data set from the Bermuda Atlantic Time series Station (BATS,  $31^\circ40'\text{N}$ ,  $64^\circ10'\text{W}$ ) (Bates, 2007) is also used as additional model validation. The addition of BATS is useful as it is one of the best studied ocean locations. For the purpose of this study, we only use data from the same period as the underway observations (i.e., 2002–2007). The data from BATS are available through the spring of 2006.

### 3 Model

In this study, we use a global coupled physical–biogeochemical ocean model (Assmann et al., 2010). The physical component is the dynamical isopycnic vertical coordinate ocean model MICOM (Bleck and Smith, 1990; Bleck et al., 1992), which includes some modifications as described in Bentsen et al. (2004). The horizontal resolution is approximately  $2.4^\circ \times 2.4^\circ$ , corresponding to grid spacing ranging from 60 km in the Arctic and Southern Ocean to 180 km in the subtropical regions. Vertically, the model consists of 34 isopycnic layers. In the additional topmost layer, the model adopts a single non-isopycnic surface mixed layer, the depth of which is computed according to formulation by Gaspar (1988). This temporally and spatially varying mixed layer provides the linkage between the atmospheric forcing and the ocean interior. The ocean carbon cycle model is the Hamburg Oceanic Carbon Cycle (HAMOCC5) model, which is based on the original work of Maier-Reimer (1993). The time step of the model is four-thirds of an hour, following the physical model. The model has since then been improved extensively and has been used in many studies (Six and Maier-Reimer, 1996; Heinze et al., 1999; Aumont et al., 2003; Maier-Reimer et al., 2005). The current version of the model includes an NPZD-type ecosystem model, a 12-layer sediment module, full carbon chemistry (Maier-Reimer et al., 2005), and multi-nutrient co-limitation of the primary production. The surface  $p\text{CO}_2$  in the model is computed based on the prognostic temperature, salinity, pressure, dissolved inorganic carbon, and alkalinity. For the air–sea gas exchange, the model adopts the formulation of Wanninkhof (1992). A detailed description of the isopycnic version of HAMOCC is given by Assmann et al. (2010).

The model simulations performed in this study are forced by the daily atmospheric fields from the NCEP Reanalysis data set (Kalnay et al., 1996). For the air–sea  $\text{CO}_2$  flux computation, the model prescribes observed atmospheric  $\text{CO}_2$  concentration (instead of the observed emissions) from Mauna Loa observatory in Hawaii, which is a reasonable proxy for global mean concentration (Gammon et al., 1985). In general, the model reproduces the amplitude and seasonal variabilities of the observed SST in all three North Atlantic locations and at BATS quite well (Supplement Fig. 1). During winter the model mixed layer depth (MLD) tends to be deeper than is observed, which may be attributed to the

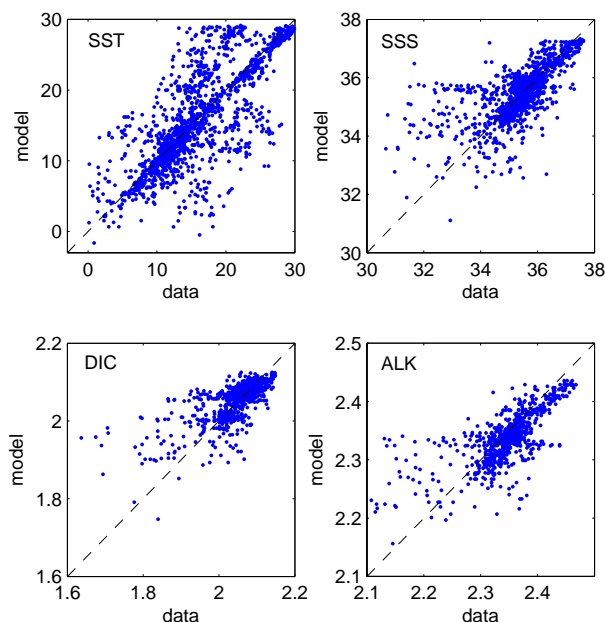
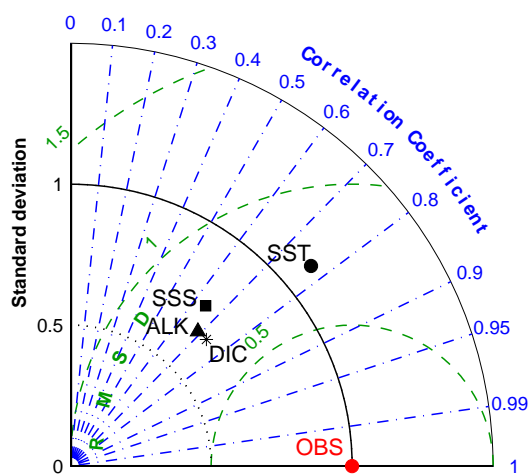


**Fig. 2.** Taylor diagramme (left panel) summarizing both the temporal (monthly) and regional (one-degree binned) model-data fit of surface temperature (SST), salinity (SSS), dissolved inorganic carbon (DIC), and alkalinity (ALK) over the North Atlantic region. The standard deviations were normalized to combine the different variables in one diagramme. The right panel shows the scatter plots comparing the model data distribution of SST ( $^{\circ}\text{C}$ ), SSS (psu), DIC ( $\text{mol m}^{-3}$ ), and ALK ( $\text{eq m}^{-3}$ ). The data are taken from a subset of the CARINA database.

slightly cooler SST as compared to the observations. A more detailed evaluation of the model performance with respect to the global physical and carbon cycle parameters is provided in Assmann et al. (2010).

## 4 Results

For the basin scale comparison with the CARINA data, the model-data fit is summarized in the Taylor diagram (Taylor et al., 2001) shown in Fig. 2. The Taylor diagram gives a statistical summary of how well the model simulated tracer distributions match the observed ones in term of correlation, standard deviations, and root-mean-square-difference (RMSD). Note that we only use the surface data set (five meter and above) for this comparison because the main focus of this manuscript is to study the surface  $p\text{CO}_2$  variability. Figure 2 shows that the model simulated range of temporal and regional variabilities are generally close to the observations. The model simulated SST, SSS, DIC and ALK distributions have significant (within 95% confidence interval) correlations of 0.77, 0.65, 0.73, and 0.69, respectively with the observations. In addition to the Taylor diagram, Fig. 2 also shows the scatter plots, which illustrate the spreads and ranges of the model simulated variables relative to those from the observation. For most of the case, there is a good agreement between the model and observation.

### 4.1 Regional seasonality of $f\text{CO}_2$

In this subsection we analyze the surface  $f\text{CO}_2$  seasonal variability for the different sub-domains in the North Atlantic. The model simulated  $p\text{CO}_2$  is converted into  $f\text{CO}_2$  by using a conversion factor of 0.3% (Weiss, 1974). This conversion is done in order to compare with data from SOCAT, which is  $f\text{CO}_2$ . Figure 3 compares the seasonal variability of surface  $f\text{CO}_2$  taken from the underway measurements as well as from the BATS station with the model simulation. For all regions, except for the Northeast Atlantic, the model broadly agrees with the observations in term of the amplitude of the seasonal cycle, but the phase is slightly shifted (e.g., in the NASPG region).

To further identify the mechanisms behind the differences in seasonal variability between the model and data, we separate the  $f\text{CO}_2$  variability into temperature-driven ( $f\text{CO}_2\text{-T}$ ) and non temperature-driven ( $f\text{CO}_2\text{-nonT}$ ) variability following Takahashi et al. (2002). The  $f\text{CO}_2\text{-T}$  represents the thermodynamic, temperature-controlled, variability, as colder water has higher  $\text{CO}_2$  solubility, thus lower  $f\text{CO}_2$ , whereas the opposite is true for warmer water. The  $f\text{CO}_2\text{-nonT}$  is composed of variability associated with alkalinity, SSS, and DIC variations throughout the year. The deviation of both the  $f\text{CO}_2\text{-T}$  and  $f\text{CO}_2\text{-nonT}$  monthly variability from the observations and model are shown in Fig. 4 for each studied region.

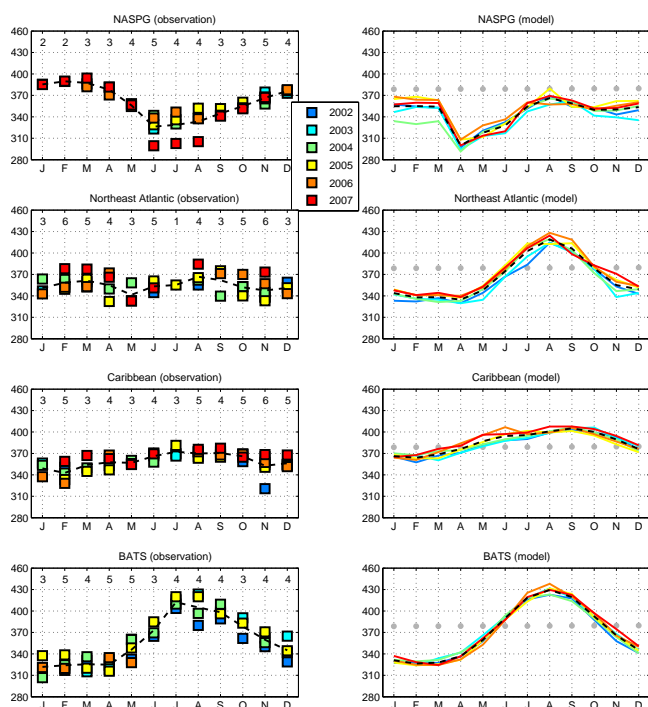


**Fig. 3.** Observed and simulated seasonal  $f\text{CO}_2$  variability (in ppm units) in the NASPG, Northeast Atlantic, Caribbean, and BATS for 2002–2007. Dashed black lines represent the mean seasonal variation. Numbers above the left-hand panels give the total number of months with observations over the 6 yr period. Grey dots in the right hand panels represent the observed monthly mean atmospheric mole fraction in dry air (in ppm units).

For the NASPG region, the observations indicate a clear seasonal signal with winter maximum and summer minimum, consistent with earlier analyses (Olsen et al., 2008) for this region. The model is in accordance with these observations, but with its seasonal phase shifted by approximately two months. Based on the observations, Olsen et al. (2008) describe that the seasonal variability in this location is mostly dominated by upward mixing of DIC-rich water to the surface in the winter and by strong biological consumption throughout spring and summer. The simulated temporal variation of mixed layer depth in this region agrees well with the climatology estimate (de Boyer Montégut et al., 2004) and ocean reanalysis product (Ferry et al., 2010), as shown in supplemental Fig. 2. Strongest mixing occurs during the winter and early spring period with maximum mixed layer depth of around 400 m depth.

Consequently, Fig. 4 shows similar observed patterns, with a weaker amplitude of the variability of  $f\text{CO}_2\text{-T}$  than  $f\text{CO}_2\text{-nonT}$  in the NASPG. The model shows good agreement with the observations in terms of  $f\text{CO}_2\text{-T}$  variability, but the amplitude of  $f\text{CO}_2\text{-nonT}$  in the model is weaker than observed. This may be attributed to the underestimated model nutrient concentration, a known weakness of the model (Assmann

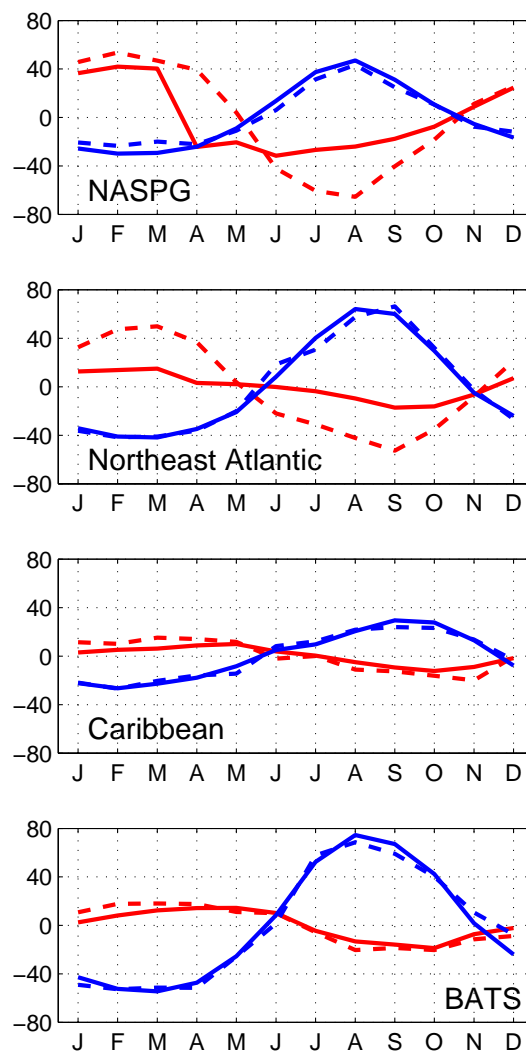


**Fig. 4.** Comparison of the mean seasonal  $f\text{CO}_2\text{-T}$  (blue) and  $f\text{CO}_2\text{-nonT}$  (red) between the model (solid-lines) and the observations (dashed-lines) for different regions in the North Atlantic.

et al., 2010). The  $f\text{CO}_2\text{-nonT}$  phase-shift in the model is predominantly attributed to the simulated timing of biological processes. In the early spring period, the increase in temperature and light availability combined with strong mixing leads to an accelerated phytoplankton growth, which is known as spring bloom. In the model, this condition immediately consumes most of the nutrient upwelled from the previous winter. As a result, the nutrients become depleted and weak nutrient regeneration over the summer season is insufficient to maintain the steady biological consumption as observed (see supplemental Fig. 3). During this period, the temperature effect simulated by the model prevails where an increase in temperature brings the simulated  $p\text{CO}_2$  back up to its high winter values (see Fig. 3). On the contrary, the observational-based study by Olsen et al. (2008) suggests



that the biological drawdown of DIC is maintained over the summer and dominates the increasing summer temperature. Consistent with the observations shown here, they found minimum  $f\text{CO}_2$  values between 325–340 ppm during the summer. Simulating the correct ecosystem dynamics at high latitudes is a well known problem in global models as most models calibrate their ecosystem model towards time-series stations such as BATS, which are biased toward the subtropical regions (Tjiputra et al., 2007). A recent one-dimensional ecosystem model study by Signorini et al. (2011) shows that more sophisticated multi-functional groups of phytoplankton may be necessary to reproduce the biological carbon uptake during summer in the Icelandic waters close to where the NASPG domain is located. In their model study, which uses three phytoplankton species parameterized individually, they show that each species thrives at different periods. For example, diatom is shown to be the dominant species in the early spring period, whereas dinoflagellates and coccolithophores play a crucial role in maintaining high summer productivity and maximizing the drawdown of surface DIC.

Our Northeast Atlantic station is located in between the North Atlantic subpolar and subtropical gyres. It is therefore expected that the variability here is dominated by both temperature variability as well as surface DIC dynamics. The observations (Fig. 4) suggest that the  $f\text{CO}_2\text{-T}$  and  $f\text{CO}_2\text{-nonT}$  variability are equally important and nearly cancel each other, resulting in the relatively weak seasonal cycle (compared to that in the sub-polar region), as shown in Fig. 3. The study by Schuster and Watson (2007) over a somewhat larger ship-based observational region ( $30^\circ\text{W}$ – $5^\circ\text{W}$  and  $39^\circ\text{N}$ – $50^\circ\text{N}$ ) also shows similar weak seasonal  $f\text{CO}_2$  variability in the early 2000s. The observations show two time intervals with maximum  $f\text{CO}_2$ : during late winter and late summer. Figure 4 shows that the late winter maximum is associated to the dynamics of surface DIC (nonT effect) whereas the late summer maximum is dominated by the temperature variations (i.e., maximum SST around the August and September months). The model is able to simulate the observed  $f\text{CO}_2\text{-T}$  seasonal cycle relatively well but the simulated  $f\text{CO}_2\text{-nonT}$  is considerably weaker. The model  $f\text{CO}_2$  variability in this location appears very similar to that at the BATS station (see Fig. 4). As described above, this artefact is potentially due to the ecosystem dynamics biased toward the one at BATS. Another explanation for the model-data mismatch is due to the coarse resolution of the model, the location of the North Atlantic current (which is important for this domain) is not correctly simulated by the model.

In the Caribbean sub-domain, both model and observations show the lowest seasonal variability of surface  $f\text{CO}_2$  as compared to the other regions (Fig. 3). This is a general feature for oligotrophic low latitude regions (e.g., Watson et al., 2009). Figure 4 shows that variations in surface temperature are the main driver for the seasonal fluctuations, consistent with an earlier observational study over the same domain (Wanninkhof et al., 2007). Consequently, the

maximum surface  $f\text{CO}_2$  occurs in the summer period when SST is high, and the minimum  $f\text{CO}_2$  is observed during winter. The smaller role of  $f\text{CO}_2\text{-nonT}$  in this location can be attributed to the relatively weak seasonal variations in both the observed chlorophyll (i.e., biological activity) and mixed layer depth (Behrenfeld et al., 2005; de Boyer Montégut et al., 2004).

A study by Bates et al. (1996) reported that the surface waters at BATS are supersaturated with respect to  $\text{CO}_2$  during the stratified summer months and undersaturated during the strong mixing in wintertime. Figure 3 shows that the model is able to simulate the observed mean seasonal cycle in terms of both phase and amplitude. While there is a pronounced seasonality in the surface DIC (i.e., upwelling of DIC-rich subsurface water mass during the winter and biological production in the summer), both the model and observations agree in that the  $f\text{CO}_2\text{-T}$  variability dominates the seasonal variations (see Fig. 4). The seasonal SST variation at BATS is as large as that in the NASPG but the seasonal Net Primary Production (NPP) cycle remains much weaker (as shown in supplemental Figs. 1 and 3). This dominant control of SST on the surface  $f\text{CO}_2$  at BATS has also been shown by Gruber et al. (2002) for the period prior to the year 2000. Thus, similar to the Caribbean station, the  $f\text{CO}_2\text{-nonT}$  at BATS has only minor contributions to the total  $f\text{CO}_2$  variation.

#### 4.2 Regional sea-air $\text{CO}_2$ flux

Here, we compare the monthly sea-air  $\text{CO}_2$  flux from the model output with the observational-based estimates. For the observed  $\text{CO}_2$  flux estimates, we use the formulation of Wanninkhof (1992) where the formulation from Weiss (1974) is used to compute the  $\text{CO}_2$  solubility. In situ SST and SSS accompanying the underway observation are used for the solubility computation. When SSS is unavailable, climatological data from the World Ocean Atlas 2009 (WOA09, Antonov et al. (2010)) is used. NCEP monthly wind speed is used to compute the gas transfer rate. Finally, the monthly atmospheric  $\text{CO}_2$  concentration observed at Mauna Loa observatory is used as a proxy for atmospheric  $p\text{CO}_2$  boundary condition over each of our stations. For the model, the  $f\text{CO}_2$  and  $\text{CO}_2$  flux variables are computed prognostically based on the simulated SST, SSS, and surface wind speed from the physical model (also based on NCEP data).

Figure 5 shows the sea-to-air  $\text{CO}_2$  flux from both the model and observations for 2002–2007. In the NASPG region, the model-data bias can largely be attributed to the differences in seasonal cycle of  $f\text{CO}_2$ . The model simulates maximum uptake during the spring season with minimum uptake during summer. On the other hand, the observational estimates show the largest uptake during late spring and summer periods with weak outgassing during the late winter period. This bias in the seasonal cycle is expected as shown earlier by the  $f\text{CO}_2$  seasonal cycle in Fig. 3. For the annual mean flux in the NASPG, the model and the

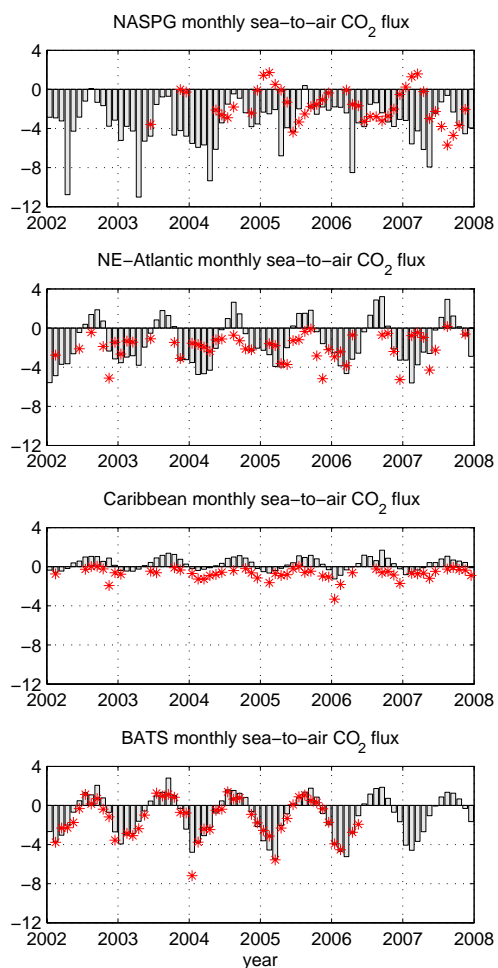


**Fig. 5.** Time-series of model simulated monthly sea-to-air  $\text{CO}_2$  flux for 2002–2007 for the NASPG, Northeast Atlantic, Caribbean and BATS stations. Whenever available, observational-based estimates are shown as well (red-stars). Positive values represent outgassing of carbon to the atmosphere and negative values represent uptake.

observations suggest net annual carbon uptakes of  $-3.5$  and  $-1.4$  moles  $\text{C m}^{-2} \text{yr}^{-1}$ , respectively. As discussed in the previous subsection, the model bias in this region can be attributed to the ecosystem module and potentially too strong winter mixing. Figure 3 also indicates that the model tends to underestimate the annual mean surface  $f\text{CO}_2$  compared to the observations.

At our Northeast Atlantic station, the model-data misfit is less than in NASPG. Note that this occurs despite the seasonal  $f\text{CO}_2$  cycles appearing very different. Both the model and observation suggest net annual carbon uptakes of  $-1.5$  and  $-1.9$  moles  $\text{C m}^{-2} \text{yr}^{-1}$ , respectively. With respect to the seasonal cycle, the observations suggest two periods with relatively strong uptake (i.e., early spring and early winter) with one period of close to neutral condition (i.e., late summer). The model only captures the strong uptake during early

spring and outgassing during late summer period. Figure 4 indicates that this seasonal bias is largely associated with the deficiencies in the model mixing and biological processes.

The model simulated sea-to-air  $\text{CO}_2$  flux seasonal cycle is in good agreement with the one calculated from the observation at the Caribbean station with weak uptake during the spring and weak outgassing in the summer. Despite this agreement, the model simulates higher monthly surface  $f\text{CO}_2$  values than the observations (see also Fig. 3), which introduces a small bias in the annual mean  $\text{CO}_2$  flux. At this location, the model suggests an annual outgassing of  $0.3$  moles  $\text{C m}^{-2} \text{yr}^{-1}$ , while the observationally based estimate suggests a net uptake of  $-0.7$  moles  $\text{C m}^{-2} \text{yr}^{-1}$ .

At the BATS station, the seasonal cycle of the sea-to-air  $\text{CO}_2$  flux from the model is in good agreement with the observations. Both estimates suggest a clear seasonality with strong carbon uptake during late winter/early spring and outgassing in the fall season. Stronger winter carbon uptake than summer outgassing shown here is also consistent with the study by Bates (2007). For the mean annual fluxes, the observationally based estimate indicates a somewhat stronger annual carbon uptake of  $-1.3$  moles  $\text{C m}^{-2} \text{yr}^{-1}$ , relative to that of the model output,  $-1.0$  moles  $\text{C m}^{-2} \text{yr}^{-1}$ . Both values are reasonable compared to the estimates from Bates (2007).

### 4.3 Regional trends in $f\text{CO}_2$ and sea-air $\text{CO}_2$ flux

In this subsection, we compare the model simulated trend with estimates from observations. Annual trends of SST, SSS, surface wind speed,  $f\text{CO}_2$ , and  $\text{CO}_2$  flux for the 2002–2007 periods were computed from the observations and model results using linear least squares methodology. The seasonal cycle in all variables is removed from both the model and observations (i.e., seasonally filtered) by subtracting the monthly mean values from the data sets.

Table 1 shows that the model and the observations consistently give trends in the same direction (increasing or decreasing) for SST and SSS, although the magnitude is weaker in the model. As described in Assmann et al. (2010), in order for the model to maintain a stable and realistic Atlantic Meridional Overturning Circulation (AMOC), a Newtonian relaxation is applied to the SST and SSS parameters in the model. For the simulation in this study, the SST and SSS are relaxed to the climatology values at time scales of 180 and 60 days, respectively. This may explain the much weaker trend simulated by the model as compared to the observations, particularly for SSS. For most stations, except BATS, warming trends are estimated by both the model and the observations. There are only small changes in the surface salinity at all stations. For the surface wind speed trend, not surprisingly, both model and observations show the same sign for all regions, as both come from the same source (i.e., NCEP Reanalysis). The discrepancies in the magnitude may be attributed to the data interpolation from NCEP to model grid domains. The seasonally filtered trends of surface  $f\text{CO}_2$  and sea-air  $\text{CO}_2$

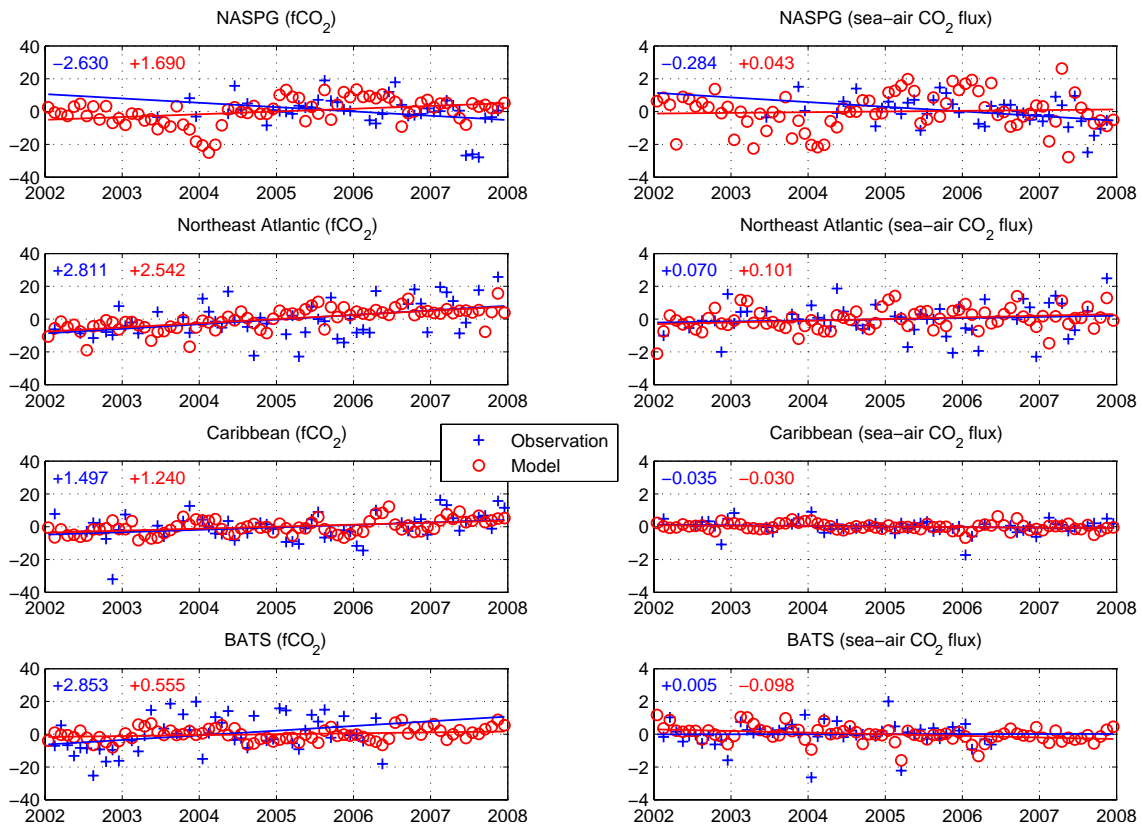


**Fig. 6.** Observed and simulated seasonally filtered (left-column) surface  $f\text{CO}_2$  and (right-column) sea-air  $\text{CO}_2$  fluxes at the NASPG, Northeast Atlantic, Caribbean, and BATS stations for 2002–2007. Units are in (ppm) and ( $\text{moles C m}^{-2} \text{ yr}^{-1}$ ), respectively. The coloured numbers represent the annual trend computed after removing the seasonal mean from both observations (blue) and model (red). Positive trend in the sea-air  $\text{CO}_2$  flux represents increasing in outgassing or less uptake, whereas negative trend represents the opposite.

fluxes at the four locations in the North Atlantic are shown in Fig. 6. After the seasonal signals are removed from the time-series, there is a clear distinction in the magnitude of the interannual variations, with higher variability being more pronounced in high latitudes. Both the model and the observations suggest that surface  $f\text{CO}_2$  interannual variability ranges within  $\pm 30$  ppm for nearly all regions. The amplitude of the interannual variability of the sea-air  $\text{CO}_2$  fluxes varies from one region to the other, with the strongest variability shown at high latitude (i.e., NASPG), and the weakest at low latitude (i.e., Caribbean).

For 2002–2007 the model shows a positive trend of surface  $f\text{CO}_2$  at all stations consistent with the observational estimates, except for the NASPG station where the observations indicate a negative trend. This is interesting as a previous study estimated that the surface  $f\text{CO}_2$  around the NASPG domain has increased relatively faster (e.g., over the period 1990–2006) than in other regions of the North Atlantic (Corbière et al., 2007; Schuster et al., 2009). The observed negative trend in the NASPG domain can be attributed to the unusually low summer  $f\text{CO}_2$  in 2007 (when the data from year 2007 is excluded, the observed  $f\text{CO}_2$  trend is

$0.502 \text{ ppm yr}^{-1}$ ), which is not reproduced by the model. This anomalously low  $f\text{CO}_2$  value is recorded despite the fact that both model and observation indicate a positive anomaly in SST (not shown) during the summer of 2007 relative to the previous summer periods, as also shown in Table 1 (i.e., a warming trend in SST). Therefore, the anomalously low summer  $f\text{CO}_2$  in 2007 may be attributed to the other factors, such as unusually high summer biological production as seen from observationally-derived estimates (Behrenfeld and Falkowski, 1997). And due to the model deficiency in maintaining high summer productivity in this location (supplement Fig. 3), it is unable to reproduce the anomalously low  $f\text{CO}_2$  value. Interestingly, a modeling study by Oschlies (2001) suggests only a small increase in the nutrient concentration in this region under a positive NAO-phase (2007 is a dominant positive NAO phase year). We note that, due to the large surface  $f\text{CO}_2$  deviation in the year 2007, a longer time series of observations is necessary to yield a more reliable long-term trend analysis.

The respective observed atmospheric  $\text{CO}_2$  trend for the same period is  $2.031 \text{ ppm yr}^{-1}$ . Due to this opposing trend, it is not surprising that the observed sea-air carbon flux in



**Table 1.** Observed seasonally filtered trends of sea surface temperature ( $^{\circ}\text{C yr}^{-1}$ ), Salinity ( $\text{psu yr}^{-1}$ ), surface wind speed ( $\text{m s}^{-1} \text{yr}^{-1}$ ), surface  $f\text{CO}_2$  ( $\text{ppm yr}^{-1}$ ), and sea-air  $\text{CO}_2$  fluxes ( $\text{mol C m}^{-2} \text{yr}^{-2}$ ) at the NASPG, Northeast Atlantic (NE-Atl.), Caribbean, and BATS stations. The numbers within parentheses represent the associated values from the model.

Parameter	NASPG	NE-Atl.	Caribbean	BATS
Period	Jan 2002–Dec 2007	Jan 2002–Dec 2007	Jan 2002–Dec 2007	Jan 2002–Dec 2007
SST	0.161 (0.047)	0.065 (0.009)	0.074 (0.065)	−0.130 (−0.072)
SSS	0.000 (0.000)	0.008 (0.001)	−0.021 (−0.014)	0.044 (0.004)
Wind	0.047 (0.023)	−0.024 (−0.063)	−0.120 (−0.068)	0.075 (0.021)
$f\text{CO}_2$	−2.630 (1.690)	2.811 (2.542)	1.497 (1.240)	2.853 (0.555)
$\text{CO}_2$ fluxes	−0.284 (0.043)	0.070 (0.101)	−0.035 (−0.030)	0.005 (−0.098)

the NASPG has a large negative trend (i.e., increasing ocean carbon uptake) of  $-0.284 \text{ mol C m}^{-2} \text{yr}^{-2}$ . The model on the other hand suggests a very small positive trend (i.e., less uptake) despite lower increase in surface ocean  $p\text{CO}_2$  ( $1.690 \text{ ppm yr}^{-1}$ ) than in atmosphere ( $2.031 \text{ ppm yr}^{-1}$ ). This can be partially attributed to the negative trend in the spring surface wind speed in the region (not shown), which leads the model to simulate weaker atmospheric carbon uptake over time. Note that for the NASPG location, the model simulates the largest sea-air  $f\text{CO}_2$  difference during the spring season as shown in Fig. 3.

At the Northeast Atlantic station, the simulated positive surface  $f\text{CO}_2$  trend of  $2.542 \text{ ppm yr}^{-1}$  compares favourably with the observed of  $2.811 \text{ ppm yr}^{-1}$ . Both the model and observations here suggest a stronger increase in oceanic  $f\text{CO}_2$  than in the atmosphere, which translates into a weak positive trend in the sea-air  $\text{CO}_2$  fluxes or less uptake (see Fig. 6). This is also consistent with the negative trend of surface wind speed (Table 1), as surface water in the Northeast Atlantic region is mostly undersaturated with respect to atmospheric  $f\text{CO}_2$  throughout the year (i.e., a net carbon sink region).

At the Caribbean station, the  $f\text{CO}_2$  trend in the model ( $1.240 \text{ ppm yr}^{-1}$ ) agrees well with the observed of  $1.497 \text{ ppm yr}^{-1}$  with magnitude weaker than the atmospheric value and therefore the sea-air  $\text{CO}_2$  fluxes are weakly decreasing (more carbon uptake). The opposing signals in  $\text{CO}_2$  fluxes between the Caribbean and the Northeast Atlantic region discussed above is also consistent with a recent observational-based estimate (covering a broader spectrum of VOS ship tracks between northwestern Europe and the Caribbean) that suggest a positive trend in carbon uptake followed by a negative one over the 2002–2007 period (Watson et al., 2009), resulting in small net change over the region.

The  $f\text{CO}_2$  trends at BATS computed from the measurements and the model are both positive. However, the signal is much stronger in the observations, resulting in a positive trend in sea-air  $\text{CO}_2$  fluxes (i.e., less oceanic uptake). The model  $f\text{CO}_2$  trend, on the other hand, is weaker than the corresponding atmospheric trend, and the model therefore simulates a negative trend of the sea-air  $\text{CO}_2$  fluxes (i.e., more

carbon uptake) in this location. Consistent with our model results, a study by Ullman et al. (2009) also suggests a relatively smaller increase in surface  $p\text{CO}_2$  at the BATS station compared to the rest of the North Atlantic region, although their trend extends over the 1992–2006 period.

#### 4.4 Basin scale trends and variability

Previous subsections show that, despite its deficiencies, the model is able to reasonably capture the seasonal variability and short-term interannual trends observed in some regions of the North Atlantic basin. Here, we attempt to explain the regional variations in the surface  $p\text{CO}_2$  trend simulated by the model and, to some extent, the observed ones. First, we analyze the dominant primary and secondary modes of long-term interannual variability of simulated surface  $p\text{CO}_2$  for 1960–2008. To do this, we first removed the mean  $p\text{CO}_2$  value from each model grid point to yield the simulated  $p\text{CO}_2$  anomaly. A principal component statistical analysis (von Storch and Zwiers, 2002) was then applied to these anomalies. Figure 7 shows the first empirical orthogonal function (EOF1) and the associated principal component (PC1) of the simulated annual surface  $p\text{CO}_2$  anomaly for 1960–2008. The first EOF explains 98% of the overall model variance. The first principal component is plotted together with anomalies of model simulated annual  $p\text{CO}_2$  and atmospheric  $\text{CO}_2$  concentration observed at the Mauna Loa station. Multiplying the EOF1 value with the PC1 time-series yields the primary mode of surface  $p\text{CO}_2$  variability simulated by the model. The temporal variability of PC1 indicates a dominant positive trend that correlates strongly with the observed atmospheric  $\text{CO}_2$  anomaly ( $r = 0.99$ ). This suggests that the primary temporal variability of surface  $p\text{CO}_2$  in the model is mainly due to the invasion of anthropogenic carbon into the seawater. Therefore, at regional scales and in the long run, the model simulated ocean  $p\text{CO}_2$  follows the atmosphere.

For the above reason, the EOF1 map shown in Fig. 7 indicates regions where the anthropogenic  $\text{CO}_2$  significantly affects the surface  $p\text{CO}_2$  concentration. The magnitude of

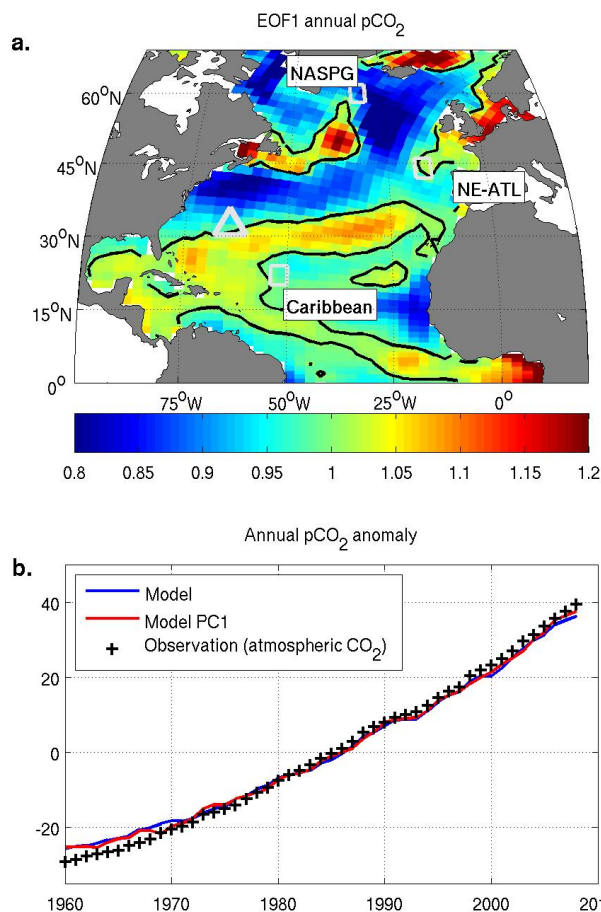


**Fig. 7.** (a) The first empirical orthogonal functions of surface  $p\text{CO}_2$  and (b) the associated principal component for 1960–2008. The black contour lines in (a) indicate the value of one. The temporal variation of PC1 in (b) is plotted together with the anomaly of model simulated annual surface  $p\text{CO}_2$  (blue line) and annual observed atmospheric  $\text{CO}_2$  concentration (black pluses).

PC1 shown in Fig. 7b is standardized to be comparable to the observed atmospheric  $\text{CO}_2$  anomaly. The EOF1 map can be used to approximate the simulated strength of increasing surface  $p\text{CO}_2$  trend over the period 1960–2008. Regions with values greater than one tend to have surface  $p\text{CO}_2$  increasing faster than regions with values less than one. Note that this trend and these variations occur over a much longer period than recent observational studies. Thus, in order to understand and compare the trend in this study with the relatively shorter trend from the observational study, a further analysis on the short term interannual climate variability is required (see below).

The main reason for the regional differences in the magnitude of the surface  $p\text{CO}_2$  increasing long-term trend can be explained in terms of the surface transport and air–sea heat flux patterns. The anthropogenic carbon taken up by the surface ocean is advected by the ocean circulation at the

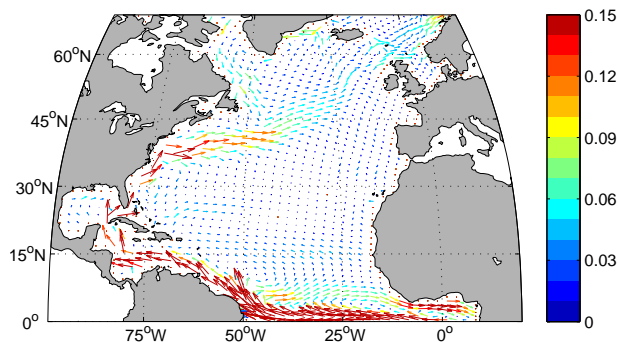


**Fig. 8.** Simulated mean North Atlantic lateral surface velocity for the period 1960–2008 ( $\text{m s}^{-1}$ ).

surface and transported into the deep by mixing and deep water formation processes (Tjiputra et al., 2010b). Figures 8 and 9 show the mean lateral ocean surface velocity and air–sea heat flux simulated by the model over the period 1960–2008. In regions with strong mass transport, such as the Gulf Stream, relatively warm water from the subtropics is advected northward and loses heat to the atmosphere. Here, the cooling of surface temperature increases the  $\text{CO}_2$  gas solubility and translates into lower surface  $p\text{CO}_2$  for the same dissolved inorganic carbon content. Thus, along 30° N and 45° N, where the water is continuously transported northeastward into the Nordic Seas by the North Atlantic drift water, the surface  $p\text{CO}_2$  increases relatively slower than most other regions, as illustrated in Fig. 7. In contrast, in the western subpolar gyre along 50° N latitude, the water mass here is transported southward from the Labrador Sea and warmed up by the atmosphere. Hence, the surface  $p\text{CO}_2$  in this region increases relatively faster than the other regions.

Consistently, a recent study by Tjiputra et al. (2010b) using a fully coupled Earth system model shows that future anthropogenic carbon uptake in the North Atlantic regions is well confined to the North Atlantic drift current region. Convergence regions such as the subtropical Atlantic convergence zone are marked by a stronger increase in surface  $p\text{CO}_2$  as less anthropogenic  $\text{CO}_2$  is laterally advected away from this area (Fig. 8) and there is a net heat gain in this region (Fig. 9). Both the Greenland and the Norwegian Seas represent some of the oldest surface water masses before they are transported to the deep water (i.e., have resided for a long period close to the sea surface), which also explains the relatively high anthropogenic  $\text{CO}_2$  concentration simulated in the model. On the western coast of North Africa, the anomalously lower contribution of anthropogenic  $\text{CO}_2$  can be explained by the fact that this is an upwelling region, where water masses unexposed to the present atmospheric  $\text{CO}_2$  concentration come to the surface.

To understand the shorter term mode variability, we compute the second mode of variability simulated by the model.

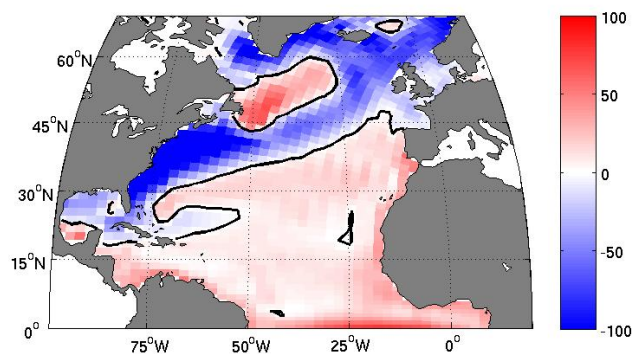


**Fig. 9.** Simulated mean North Atlantic air–sea heat fluxes for the period 1960–2008 ( $\text{W m}^{-1}$ ). The black contour lines indicate the value of zero.

Figure 10 shows the EOF2, which gives the dominant variability of surface  $p\text{CO}_2$  after the positive trend resulting from the anthropogenic  $\text{CO}_2$  uptake (see Fig. 7b) is removed. Thus it explains the main variations due to physical climate variability over the period 1960–2008. Figure 10b shows that the temporal variations of PC2 are reasonably well correlated with the North Atlantic Oscillation (NAO)-index (Hurrell and Deser, 2009) ( $r = 0.557$ ). The NAO is a leading climate variability pattern over the North Atlantic, which affects, e.g., the heat content and circulation of the ocean. The correlation is stronger during strong NAO index events (i.e., when the NAO-index is greater than one standard deviation,  $r = 0.747$ ). This correlation of  $p\text{CO}_2$  and NAO variability is consistent with a previous study (Thomas et al., 2008), which shows that changes in wind-driven surface ocean circulation associated with the NAO variability influence the North Atlantic  $\text{CO}_2$  system.

The spatial pattern of EOF2 shown in Fig. 10 indicates that the second mode of variability (approximately NAO-like) predominantly represents the interannual variability of surface  $p\text{CO}_2$  in the North Atlantic sub-polar region, with opposite variability between the western and eastern parts. In the western sub-polar gyre, the model simulates negative anomalies of  $p\text{CO}_2$  under positive NAO conditions, whereas positive anomalies are simulated in the eastern part of the sub-polar gyre.

In the model, the  $p\text{CO}_2$  is determined as a function of surface temperature (SST), salinity (SSS), alkalinity, and dissolved inorganic carbon (DIC) concentrations. To quantify the influence of the NAO-variability on each of these parameters, we analyzed an earlier model simulation, which used the same atmospheric physical forcing, but maintained a preindustrial atmospheric  $\text{CO}_2$  concentration (Assmann et al., 2010). This simulation, in principle, would have the positive  $p\text{CO}_2$  trend associated with the anthropogenic effects, as shown in Fig. 7, removed from the system. Therefore, it can be better used to analyze the variability of the  $\text{CO}_2$  system associated with the present climate variability. Next,

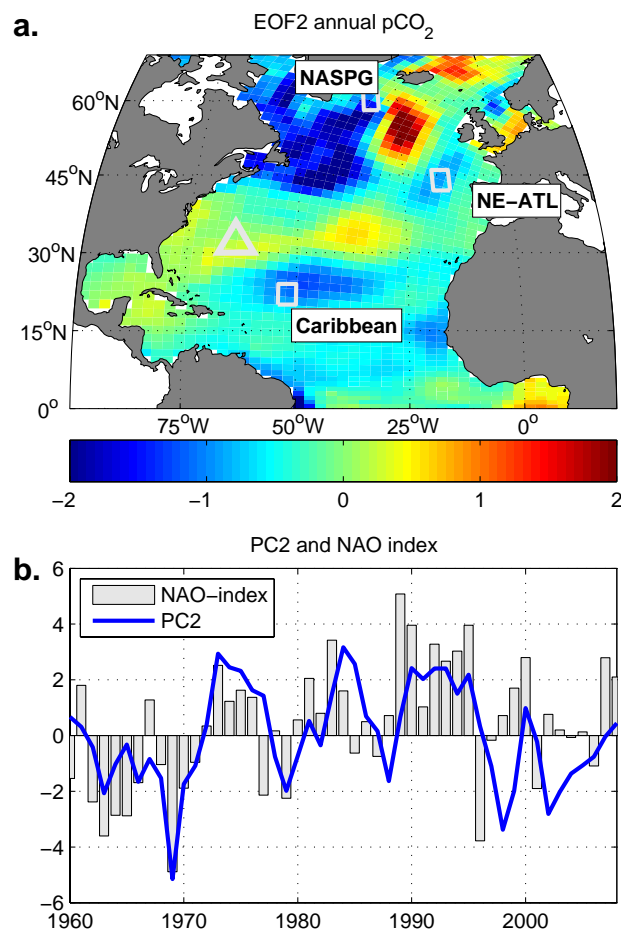


**Fig. 10.** (a) The second empirical orthogonal function of surface  $p\text{CO}_2$  and (b) the associated principal component (blue line) together with the observed North Atlantic Oscillation index (grey bars) for 1960–2008.

we compute mean annual anomalies of the simulated SST, SSS, alkalinity, and DIC under the dominant positive and negative NAO phases between 1960–2007. The dominant NAO-phase is defined here as years when the absolute NAO-index is larger than one standard deviation. The computed annual anomalies are then used to construct a composite of the surface  $p\text{CO}_2$  anomalies attributed to changes in these parameters under both positive and negative NAO condition, as shown in Fig. 11. For example, to compute the SST-attributed  $p\text{CO}_2$  anomaly (i.e.,  $p\text{CO}_2\text{-SST}$ ), we compute the  $p\text{CO}_2$  applying the SST anomalies together with the mean values of SSS, alkalinity, and DIC simulated by the model. For the  $p\text{CO}_2$  computation here, we use the Matlab code provided by Zeebe and Wolf-Gladrow (2001).

In the North Atlantic, the surface temperature has been recognized to vary with respect to the dominant NAO variability (Hurrell and Deser, 2009). The model simulates well the expected tri-polar SST anomalies that are direct result of

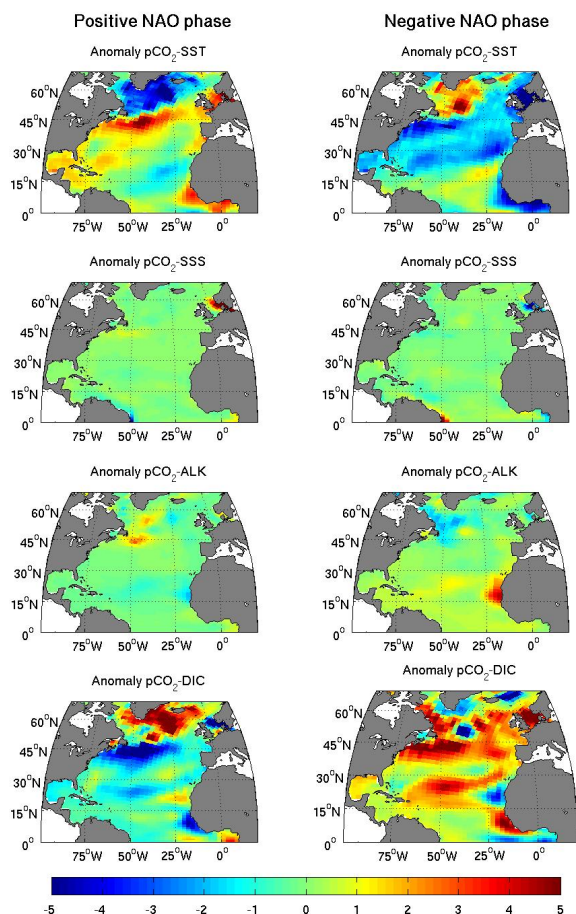


**Fig. 11.** Composites of annual surface  $p\text{CO}_2$  anomalies associated with changes in surface temperature, salinity, alkalinity, and dissolved inorganic carbon under a dominant positive and negative phase of the North Atlantic Oscillation. Years with dominant positive and negative NAO phases are defined as the year when the winter (December–March) NAO-index is greater and smaller than one standard deviation computed over the period 1960–2008, respectively. Units are in ppm.

the anomalous air–sea heat fluxes associated with the different NAO-modes (Marshall et al., 2001). These have been shown to persist for about a year (Watanabe and Kimoto, 2000). Under a positive NAO-mode, the tri-polar structure consists of the following: a cold anomaly in the subpolar North Atlantic due to the enhanced northerly cold Arctic air masses, which results in net sea-to-air heat loss, and in the mid-latitudes, stronger westerly flows introduce relatively warm air mass and creating a warm anomaly in the region. A strong correlation between the SST and NAO-index in the North Sea is also shown, due to the NAO-dependent inflow of warmer and more saline Atlantic water mass into the region (Pingree, 2005) which is also reflected in the  $p\text{CO}_2$ -SSS component in Fig. 11. Finally, stronger

clockwise flow over the subtropical Atlantic high leads to a negative SST anomaly, which closes the tri-polar structure. During the negative NAO-mode, the approximately opposite conditions prevail. Figure 11 shows that this regional change in SST translates into similar regional variability in the surface  $p\text{CO}_2$  anomalies, with colder SST yielding negative  $p\text{CO}_2$  anomalies whereas warmer SSTs yield the opposite. The strongest NAO-associated temperature effect on the surface  $p\text{CO}_2$  occurs in the western part of the North Atlantic subpolar gyre. This region has been recently shown by Corbière et al. (2007) and Metzl et al. (2010) to have a positive trend in surface  $p\text{CO}_2$ , predominantly attributed by the observed surface warming. For a similar period as their studies, i.e., 1993–2008, our model also simulates a surface  $p\text{CO}_2$  trend between 2.0 and 2.5 ppm yr<sup>-1</sup> in the same region. Figure 10 shows that the surface  $p\text{CO}_2$  in this region (between Iceland and Northeastern Canada) is reasonably well (negatively) correlated with the NAO-index. The NAO-phase is moving from dominant positive (year 1993) into more neutral phase (year 2000 and 2001) and from weak negative (year 2001) to positive phase (year 2008). Thus we could expect to have increasing  $p\text{CO}_2$  due to temperature variations at the former stage follow by DIC variations at the latter stage. Other regions strongly affected by the temperature variability, such as the eastern part of the subpolar gyre and along the North Atlantic drift region, are damped by the opposing  $p\text{CO}_2$ -DIC variability, as described below.

Due to the relaxation applied to the SSS in the model, the year-to-year salinity variations are weak. Therefore, the salinity in the model has relatively small effect than the other parameters in influencing the surface  $p\text{CO}_2$  over most of the North Atlantic basin. A weak positive SSS anomaly during a strong positive NAO phase is simulated in the western part of the transition region between the subtropical and subpolar gyre (slightly south of 45° N), which is associated to the northward shift of the subtropical gyre transporting more saline water from the tropics. The opposite is seen during a negative NAO phase.

The variability of surface  $p\text{CO}_2$  due to variations of alkalinity in the surface is generally small (Tjiputra and Wiguth, 2008). Figure 11 shows that under both dominant NAO-phases the  $p\text{CO}_2$ -ALK variability is most pronounced along the western coast of North Africa. Close to the North African coast, anomalously high trade winds during positive NAO phase (Visbeck et al., 2003) lead to enhanced nutrient upwelling and surface biological production. This is consistent with a study by Oschlies (2001), which shows that surface nutrient input in this region is enhanced by both vertical mixing and horizontal advection during dominant positive NAO phases. This NPP increase explains the lower  $p\text{CO}_2$ -alkalinity as biological production increases surface alkalinity through nitrate consumption, and thus reduces the  $p\text{CO}_2$ . Note that the calcification process in the model also reduce the alkalinity, but less significant than nitrate consumption.



The DIC driven surface  $p\text{CO}_2$  variability is very pronounced along the North Atlantic inter-gyre boundary region located along  $45^\circ\text{N}$  (i.e., between the North Atlantic subtropical and subpolar gyres). Stronger wind-forced surface water transport during a positive NAO phase leads to an increase in supply of relatively low-DIC subtropical water, which induces a negative annual anomaly of  $p\text{CO}_2$ -DIC. The reverse is true for dominant negative NAO phase years. In the northeastern part of the North Atlantic subpolar gyre (i.e., approximately between  $55^\circ\text{N}$ – $60^\circ\text{N}$  and  $25^\circ\text{W}$ – $30^\circ\text{W}$ ), strong cooling under a positive NAO phase deepens the winter MLD and upwells DIC-rich deep water, creating a positive  $p\text{CO}_2$ -DIC anomaly. In contrast, Thomas et al. (2008) show a negative  $\Delta p\text{CO}_2$  (reduced surface  $p\text{CO}_2$ ) in this region during the early 1990s positive NAO period due to an increase in low-DIC water mass from the subtropical region. This disagreement may be attributed to the difference in the location of the North Atlantic drift simulated by the different models. In the southern part of the subpolar gyre (i.e., centered approximately around  $50^\circ\text{N}$  and  $38^\circ\text{W}$ ), the  $p\text{CO}_2$ -DIC shows distinct variations between the two phases of NAO. Under dominant positive NAO years, a stronger southward current from the Labrador Sea transports colder (as also shown in  $p\text{CO}_2$ -SST), DIC-rich water and leads to a positive  $p\text{CO}_2$ -DIC anomaly. Under a dominant negative NAO-phase, the model shows a clear opposite regional pattern. There is also a pronounced co-variation between the NAO and the  $p\text{CO}_2$ -DIC in the center of the subtropical gyre. Visbeck et al. (2003) show that the winter wind stress in this location is co-varying with the NAO, which is attributed to the slightly enhanced trade winds during positive NAO conditions. In the model, this relation translates into stronger surface DIC transport away from the region, creating a negative  $p\text{CO}_2$ -DIC anomaly. Consequently, the model also simulates a positive air–sea  $\text{CO}_2$  flux anomaly (i.e., more carbon uptake) in this location during a dominant positive NAO phase (not shown). During a negative NAO phase, the opposite process occurs. Figure 10 shows that the DIC control of surface  $p\text{CO}_2$  in the inter-gyre boundary is damped by the SST effect. Similarly, in the southern part of the subpolar gyre the  $p\text{CO}_2$ -SST overcomes the  $p\text{CO}_2$ -DIC variability. The strongest effects of  $p\text{CO}_2$ -DIC variability due to changes in the NAO-phase are taking effect in the eastern subpolar gyre and in the central subtropical gyre.

#### 4.5 Monitoring future feedback

Figure 1 shows that there are in particular three locations representing different oceanographic provinces away from the continental margins in the North Atlantic, where the frequency of underway  $f\text{CO}_2$  measurements shows full seasonal cycles over multiple years in a relatively small area. This is mostly due to the operation of autonomous  $p\text{CO}_2$  instruments on well-established shipping lines between Europe and North America (Pfeil et al., 2012) and the fact that

underway  $p\text{CO}_2$  observations are relatively cost efficient to obtain compared to the traditional bottle data. It is not up to the  $\text{CO}_2$  research community to decide the routes of commercial vessels and while these locations are not optimal (i.e., as suggested by our model), if the measurements are continued steadily, they may have the potential to monitor any emerging climate feedback on carbon uptake in the future. In both Figs. 7a and 10a, these three locations show that surface ocean  $p\text{CO}_2$  generally increases at a rate following the atmospheric  $\text{CO}_2$  increase (i.e., value close to one in Fig. 7a) but with short term deviations that depends on the NAO variability. Therefore, continued measurements on these lines will be useful to better constrain any short term change in the surface  $p\text{CO}_2$  trend recently observed in parts of the North Atlantic. For example, a recent study by Metzl et al. (2010) shows that observations of surface  $p\text{CO}_2$  between Iceland and Canada over the 1993–2008 indicate an positive trend faster than the atmosphere. This is consistent with Fig. 10, which shows that the region has a negative correlation with the NAO index, and over the 1993–2008 the NAO index trend is negative.

To evaluate the expected carbon system response at the three regions we identified in the SOCAT data as well as at BATS, the model is applied to compute the  $p\text{CO}_2$  trend at each location during relatively large shifts of NAO regimes. We focus on two periods: one with a strong shift from negative to positive (1969–1973) and one from positive to negative (1993–1997) NAO-index (see Fig. 10b). Table 2 summarizes the trends in surface  $p\text{CO}_2$  as well as the sea-air  $\text{CO}_2$  fluxes simulated by the model. During the 1969–1973 period of strong positive trend of NAO (strong shift from negative to positive), the NASPG, Northeast Atlantic, and Caribbean stations have weaker  $p\text{CO}_2$  trends than the atmosphere. The trend at BATS more closely follows the atmospheric trend. Analogously, the model also simulates a negative  $\text{CO}_2$  flux trend (more carbon uptake) in the NASPG and the Caribbean, whereas less carbon uptake (or more outgassing) is simulated at BATS. Interestingly, the model simulates a weak increase in outgassing (less uptake) in the Northeast Atlantic location. Since the model does not perform well compared to the observation in this location (see Figs. 3 and 4), it is more difficult to interpret the results. During the positive to negative shifts in the NAO index (1993–1997), the model shows the opposite signals, but with much stronger trends in surface  $p\text{CO}_2$  at the three underway stations relative to the atmospheric  $\text{CO}_2$  trend. Consequently, the sea-air  $\text{CO}_2$  fluxes show positive trends (less uptake) for these locations. For the BATS station, our model shows the opposite signals (i.e., negative sea-air  $\text{CO}_2$  fluxes trend) for this period. This is consistent with earlier study by Gruber et al. (2002) who also show a dominant negative trend in  $\text{CO}_2$  fluxes (more carbon uptake) for the period 1993–1997.



**Table 2.** Seasonally filtered surface  $p\text{CO}_2$  and sea-air  $\text{CO}_2$  fluxes trends from the model at the NASPG, Northeast Atlantic, Caribbean, and BATS stations for the periods 1969–1973 and 1993–1997. Positive trends for the sea-air  $\text{CO}_2$  fluxes indicate less uptake, and negative ones indicate more. The atmospheric  $\text{CO}_2$  trend is computed from the Mauna Loa data.

Periods	NASPG	NE-Atl.	Caribbean	BATS	atm. $\text{CO}_2$
$p\text{CO}_2$ trend ( $\text{ppm yr}^{-1}$ )					
1969–1973	–0.392	0.449	–0.404	0.965	1.141
1993–1997	2.768	2.834	2.730	0.2396	1.610
$\text{CO}_2$ fluxes trend ( $\text{moles C m}^{-2} \text{ yr}^{-2}$ )					
1969–1973	–0.110	0.007	–0.075	0.054	
1993–1997	0.255	0.089	0.0336	–0.0582	

## 5 Summary

In this study, we use a coupled ocean biogeochemical general circulation model to assess the long term variability of surface  $f\text{CO}_2$  in the North Atlantic. We apply two independent data sets to validate the model simulation (CARINA and SOCAT). For most of the locations we select, the model is able to produce the correct amplitude of the observed seasonal cycle. In the North Atlantic subpolar gyre, the seasonal cycle phase in the model is slightly shifted compared to the observations, which can be attributed to the model deficiency in the surface biological processes. Additionally, the model broadly agrees with the observation in the interannual trend of surface  $f\text{CO}_2$  and air–sea  $\text{CO}_2$  fluxes.

Using a principal component analysis, we show that the primary variability of the surface  $p\text{CO}_2$  simulated by the model over the period 1960–2008 is associated with the increasing trend of atmospheric  $\text{CO}_2$ . The spatial variability of this trend is predominantly influenced by the surface ocean circulation and air–sea heat flux patterns. Regions with steady mass transport or heat loss to the atmosphere, such as the North Atlantic drift current, generally have weaker  $p\text{CO}_2$  trends than most other regions. In contrast, convergence regions (e.g., subtropical gyres) or regions with large heat gain (e.g., western subpolar gyre) have a relatively larger trend over the long-term period.

The analysis also reveals that over shorter interannual to decadal time scales, the variability of surface  $p\text{CO}_2$  is considerably influenced by the NAO, the leading climate variability pattern over the North Atlantic. We also evaluate the physical and chemical mechanisms behind the NAO induced regional  $p\text{CO}_2$  variations. The NAO associated temperature variability influences the surface  $p\text{CO}_2$  variability, particularly in the western part of the subpolar gyre. In the inter-gyre boundary, the  $p\text{CO}_2$  variations due to change in SST and DIC are almost equal in magnitude but in opposite directions, so they cancel each other. In the subtropical gyre, the change in wind stress in different NAO-regimes affects the transport of surface DIC, and hence alters the surface  $p\text{CO}_2$ .

In general we find very little contributions from SSS and alkalinity to the overall  $p\text{CO}_2$  variability.

Based on the model analysis, regions where the surface carbon system variability is strongly influenced by the NAO (e.g., the subpolar gyre) generally do not have sufficient temporal coverage. Nevertheless, we show that, while not optimal, if the currently established shipping routes in the North Atlantic continue to record the surface  $p\text{CO}_2$ , they will have the potential to monitor any long term  $p\text{CO}_2$  variability as well as solidify our understanding of climate-carbon cycle interactions in the North Atlantic basin. Note also that the SOCAT data capacity is beyond what is shown in this study. The growing SOCAT database can also be applied to map the climatology state in the North Atlantic as well as to evaluate model performance by applying data assimilation.

Presently, the next generation MICOM–HAMOCC model is being tested. The latest version of the model adopts a higher spatial resolution, improved physical mixing parameterization, as well as updated carbon chemistry. Together with more publicly available underway  $f\text{CO}_2$  data that is soon to be released (SOCATv2), we intend to perform a similar study to further evaluate the model–data inconsistencies. Improving the ecosystem parameterization in the model, which is shown here to be one of the model deficiencies at high latitude, through data assimilation method is also on the agenda.

**Supplementary material related to this article is available online at: <http://www.biogeosciences.net/9/907/2012/bg-9-907-2012-supplement.pdf>.**

*Acknowledgements.* We thank Richard Bellerby for reviewing the early version of the manuscript. The authors also thank both anonymous referees for their feedback which improved the manuscript considerably. This study at the University of Bergen and Bjerknes Centre for Climate Research is supported by the Research Council of Norway funded projects CarboSeason (185105/S30) and A-CARB (188167) and by the European Commission through funds from the EU FP7 Coordination Action Carbon Observing

System COCOS (212196). We also acknowledge the Norwegian Metacenter for Computational Science and Storage Infrastructure (NOTUR and Norstore, “Biogeochemical Earth system modeling” project nn2980k and ns2980k) for providing the computing and storage resources. This is publication no. A391 from the Bjerknes Centre for Climate Research.

Edited by: X. Wang

## References

- Antonov, J. I., Seidov, D., Boyer, P. T., Locarnini, R. A., Mishonov, A. V., Garcia, H. E., Baranova, O. K., Zweng, M. M., and Johnson, D. R.: World Ocean Atlas 2009, Volume 2: Salinity, edited by: Levitus, S., NOAA Atlas NESDIS 69, U.S. Government Printing Office, Washington, D. C., 184 pp., 2010.
- Assmann, K. M., Bentsen, M., Segschneider, J., and Heinze, C.: An isopycnic ocean carbon cycle model, *Geosci. Model Dev.*, 3, 143–167, doi:10.5194/gmd-3-143-2010, 2010.
- Aumont, O., Maier-Reimer, E., Blain, S., and Monfray, P.: An ecosystem model of the global ocean including Fe, Si, P colimitations, *Global Biogeochem. Cy.*, 17, 1060, doi:10.1029/2001GB001745, 2003.
- Bates, N. R.: Interannual variability of the oceanic  $\text{CO}_2$  sink in the subtropical gyre of the North Atlantic Ocean over the last 2 decades, *J. Geophys. Res.*, 112, C09013, doi:10.1029/2006JC003759, 2007.
- Bates, N. R., Michaels, A. F., and Knap, A. H.: Seasonal and interannual variability of the oceanic carbon dioxide system at the US JGOFS Bermuda Atlantic Time-series Site, *Deep-Sea Res. Pt. II*, 43, 347–383, 1996.
- Behrenfeld, M. J. and Falkowski, P. G.: Photosynthetic rates derived from satellite-based chlorophyll concentration, *Limnol. Oceanogr.*, 42, 1–20, 1997.
- Behrenfeld, M. J., Boss, E., Siegel, D. A., and Shea, D. M.: Carbon-based ocean productivity and phytoplankton physiology from space, *Global Biogeochem. Cy.*, 19, GB1006, doi:10.1029/2004GB002299, 2005.
- Bennington, V., McKinley, G. A., Dutkiewicz, S., and Ullman, D.: What does chlorophyll variability tell us about export and air–sea  $\text{CO}_2$  flux variability in the North Atlantic?, *Global Biogeochem. Cy.*, 23, GB3002, doi:10.1029/2008GB003241, 2009.
- Bentsen, M., Drange, H., Furevik, T., and Zhou, T.: Simulated variability of the Atlantic meridional overturning circulation, *Clim. Dynam.*, 22, 701–720, 2004.
- Bleck, R. and Smith, L. T.: A wind-driven isopycnic coordinate model of the North and Equatorial Atlantic Ocean. 1. Model development and supporting experiments, *J. Geophys. Res.*, 95, 3273–3285, 1990.
- Bleck, R., Rooth, C., Hu, D., and Smith, L. T.: Salinity-driven thermocline transients in a wind- and thermohaline-forced isopycnic coordinate model of the North Atlantic, *J. Pys. Oceanogr.*, 22, 1486–1505, 1992.
- de Boyer Montégut, C., Madec, G., Fischer, A. S., Lazar, A., and Iudicone, D.: Mixed layer depth over the global ocean: an examination of profile data and a profile-based climatology, *J. Geophys. Res.*, 109, C12003, doi:10.1029/2004JC002378, 2004.
- Canadell, J. G., Le Quéré, C., Raupach, M. R., Field, C. B., Buitenhuis, E. T., Ciais, P., Conway, T. J., Gillett, N. P., Houghton, R. A., and Marland, G.: Contributions to accelerating atmospheric  $\text{CO}_2$  growth from economic activity, carbon intensity, and efficiency of natural sinks, *P. Natl. Acad. Sci. USA*, 104, 18866–18870, 2007.
- Corbière, A., Metzl, N., Reverdin, G., Brunet, C., and Takahashi, T.: Interannual and decadal variability of the oceanic carbon sink in the North Atlantic subpolar gyre, *Tellus B*, 59, 168–179, doi:10.1111/j.1600-0889.2006.00232.x, 2007.
- Ferry, R., Parent, L., Garric, G., Barnier, B., Jourdain, P., and the Mercator Ocean team: Mercator Global Eddy Permitting Ocean Reanalysis GLORYS1V1: Description and Results, *Mercator Ocean Quarterly Newsletter*, 36, 11–27, , 2010.
- Gammon, R., Sundquist, E., and Frazer, P.: History of carbon dioxide in the atmosphere, in atmospheric carbon dioxide and the global carbon cycle, Rep. DOE/ER-0239, US Dep. of Energy, Washington DC, 1985.
- Gaspar, P.: Modeling the seasonal cycle of the upper ocean, *J. Phys. Oceanogr.*, 18, 161–180, 1988.
- González Dávila, M., Santana-Casiano, J. M., Merlivat, L., Barbero-Muñoz, L., and Dafner, E. V.: Fluxes of  $\text{CO}_2$  between the atmosphere and the ocean during the POMME project in the Northeast Atlantic Ocean during 2001, *J. Geophys. Res.*, 110, C07S11, doi:10.1029/2004JC002763, 2005.
- Gruber, N., Keeling, C. D., and Bates, N. R.: Interannual variability in the North Atlantic ocean carbon sink, *Science*, 298, 2374–2378, 2002.
- Heinze, C., Maier-Reimer, E., Winguth, A. M. E., and Archer, D.: A global oceanic sediment model for long-term climate studies, *Global Biogeochem. Cy.*, 13, 221–250, 1999.
- Hurrell, J. W. and Deser, C.: North Atlantic climate variability: the role of the North Atlantic Oscillation, *J. Mar. Syst.*, 78, 28–41, doi:10.1016/j.jmarsys.2008.11.026, 2009.
- Kalnay, E., Kanamitsu, M., Kistler, R., Collins, W., Deaven, D., Gandin, L., Iredell, M., Saha, S., White, G., Woollen, J., Zhu, Y., Chelliah, M., Ebisuzaki, W., Higgins, W., Janowiak, J., Mo, K. C., Ropelewski, C., Wang, J., Leetmaa, A., Reynolds, R., Jenne, R., and Joseph, D.: The NCEP/NCAR 40-yr reanalysis project, *B. Am. Meteorol. Soc.*, 77, 437–471, 1996.
- Key, R. M., Tanhua, T., Olsen, A., Hoppema, M., Jutterström, S., Schirnick, C., van Heuven, S., Kozyr, A., Lin, X., Velo, A., Wallace, D. W. R., and Mintrop, L.: The CARINA data synthesis project: introduction and overview, *Earth Syst. Sci. Data*, 2, 105–121, doi:10.5194/essd-2-105-2010, 2010.
- Lee, K., Tong, L. T., Millero, F. J., Sabine, C. L., Dickson, A. G., Goyet, C., Park, G.-H., Wanninkhof, R., Feely, R. A., and Key, R. M.: Global relationships of total alkalinity with salinity and temperature in surface waters of the world’s oceans, *Geophys. Res. Lett.*, 33, L19605, doi:10.1029/2006GL027207, 2006.
- Lefèvre, N., Watson, A. J., Olsen, A., Rios, A. F., Pérez, F. F., and Johannessen, T.: A decrease in the sink for atmospheric  $\text{CO}_2$  in the North Atlantic, *Geophys. Res. Lett.*, 31, L07306, doi:10.1029/2003GL018957, 2004.
- Le Quéré, C., Raupach, M. R., Canadell, J. G., Marland, G., Bopp, L., Ciais, P., Conway, T. J., Doney, S. C., Feely, R., Foster, P., Friedlingstein, P., Gurney, K., Houghton, R. A., House, J. I., Huntingford, C., Levy, P. E., Lomas, M. R., Mankut, J., Metzl, N., Ometto, J. P., Peters, G. P., Prentice, I. C.,

- Randerson, J. T., Running, S. W., Sarmiento, J. L., Schuster, U., Sitch, S., Viovy, T. T. N., van der Werf, G. R., and Woodward, F. I.: Trends in the sources and sinks of carbon dioxide, *Nat. Geosci.*, 2, 831–836, doi:10.1038/ngeo689, 2009.
- Levine, N. M., Doney, S., Lima, I., Wanninkhof, R., Bates, N. R., and Feely, R.: The impact of the North Atlantic Oscillation on the uptake and accumulation of anthropogenic  $\text{CO}_2$  by North Atlantic Ocean mode waters, *Global Biogeochem. Cy.*, 25, GB3022, doi:10.1029/2010GB003892, 2011.
- Lüger, H., Wanninkhof, W., Wallace, D. W. R., and Körtzinger, A.:  $\text{CO}_2$  fluxes in the subtropical and subarctic North Atlantic based on measurements from a volunteer observing ship, *J. Geophys. Res.*, 111, C06024, doi:10.1029/2005JC003101, 2006.
- Maier-Reimer, E.: Geochemical cycles in an ocean general circulation model, preindustrial tracer distributions, *Global Biogeochem. Cy.*, 7, 645–677, 1993.
- Maier-Reimer, E., Kriest, I., Segschneider, J., and Wetzel, P.: The Hamburg Ocean Carbon Cycle Model HAMOCC5.1 – Technical Description Release 1.1, Berichte zur Erdsystemforschung 14, ISSN 1614–1199, Max Planck Institute for Meteorology, Hamburg, Germany, 50 pp., 2005.
- Marshall, J., Kushnir, Y., Batisti, D., Chang, P., Czaja, A., Dickson, R., Hurrell, J., McCartney, M., Saravanan, R., and Visbeck, M.: North Atlantic climate variability; phenomena, impacts and mechanisms, *Int. J. Climatol.*, 21, 1863–1898, 2001.
- McKinley, G. A., Fay, A. R., Takahashi, T., and Metzl, N.: Convergence of atmospheric and North Atlantic carbon dioxide trends on multidecadal timescales, *Nat. Geosci.*, 4, 606–610, doi:10.1038/ngeo1193, 2011.
- Metzl, N., Corbière, A., Reverdin, G., Lenton, A., Takahashi, T., Olsen, A., Johannessen, T., Pierrot, D., Wanninkhof, R., Ólafsdóttir, S. R., Ólafsson, J., and Ramonet, M.: Recent acceleration of the sea surface  $f\text{CO}_2$  growth rate in the North Atlantic subpolar gyre (1993–2008) revealed by winter observations, *Global Biogeochem. Cy.*, 24, GB4004, doi:10.1029/2009GB003658, 2010.
- Olsen, A., Brown, K. R., Chierici, M., Johannessen, T., and Neill, C.: Sea-surface  $\text{CO}_2$  fugacity in the subpolar North Atlantic, *Biogeosciences*, 5, 535–547, doi:10.5194/bg-5-535-2008, 2008.
- Oschlies, A.: NAO-induced long-term changes in nutrient supply to the surface waters of the North Atlantic, *Geophys. Res. Lett.*, 28, 1751–1754, 2001.
- Padin, X. A., Vázquez-Rodríguez, M., Castaño, M., Velo, A., Alonso-Pérez, F., Gago, J., Gilcoto, M., Álvarez, M., Pardo, P. C., de la Paz, M., Ríos, A. F., and Pérez, F. F.: Air-Sea  $\text{CO}_2$  fluxes in the Atlantic as measured during boreal spring and autumn, *Biogeosciences*, 7, 1587–1606, doi:10.5194/bg-7-1587-2010, 2010.
- Pfeil, B., Olsen, A., and Bakker, D. C. E.: A uniform, quality controlled Surface Ocean  $\text{CO}_2$  Atlas (SOCAT), *Earth Syst. Sci. Data*, in preparation, 2012.
- Pierrot, D., Neill, C., Sullivan, K., Castle, R., Wanninkhof, R., Lüger, H., Johannessen, T., Olsen, A., Feely, R. A., and Cosca, C. E.: Recommendations for autonomous underway  $p\text{CO}_2$  measuring systems and data-reduction routines, *Deep-Sea Res. Pt. II*, 56, 512–522, doi:10.1016/j.dsr2.2008.12.005, 2009.
- Pierrot, D., Brown, P., Van Heuven, S., Tanhua, T., Schuster, U., Wanninkhof, R., and Key, R. M.: CARINA  $\text{TCO}_2$  data in the Atlantic Ocean, *Earth Syst. Sci. Data*, 2, 177–187, doi:10.5194/essd-2-177-2010, 2010.
- Pingree, R.: North Atlantic and North Sea climate change: curl up, shut down, NAO and ocean colour, *J. Mar. Biol. Ass. UK*, 85, 1301–1315, 2005.
- Schuster, U. and Watson, A. J.: A variable and decreasing sink for atmospheric  $\text{CO}_2$  in the North Atlantic, *J. Geophys. Res.*, 112, C11006, doi:10.1029/2006JC003941, 2007.
- Schuster, U., Watson, A. J., Bates, N. R., Corbière, A., Gonzales-Davila, M., Metzl, N., Pierrot, D., and Santana-Casiano, M.: Trends in North Atlantic sea-surface  $f\text{CO}_2$  from 1990 to 2006, *Deep-Sea Res. Pt. II*, 56, 620–629, doi:10.1016/j.dsr2.2008.12.011, 2009.
- Signorini, S. R., Häkkinen, S., Gudmundsson, K., Olsen, A., Omar, A. M., Ólafsson, J., Reverdin, G., Henson, S. A., and McClain, C. R.: The role of phytoplankton dynamics in the seasonal variability of carbon in the subpolar North Atlantic – a modeling study, *Geosci. Model Dev. Discuss.*, 4, 289–342, doi:10.5194/gmdd-4-289-2011, 2011.
- Six, K. D. and Maier-Reimer, E.: Effects of plankton dynamics on seasonal carbon fluxes in an ocean general circulation model, *Global Biogeochem. Cy.*, 10, 559–583, 1996.
- Steinhoff, T.: Carbon and nutrient fluxes in the North Atlantic, Ph.D. thesis, Christian-Albrechts-Universität zu Kiel, Kiel, Germany, 162 pp., 2010.
- Takahashi, T., Sutherland, S. C., Sweeney, C., Poisson, A., Metzl, N., Tilbrook, B., Bates, N., Wanninkhof, R., Feely, R. A., Sabine, C., Ólafsson, J., and Nojiri, Y.: Global sea-air  $\text{CO}_2$  flux based on climatological surface ocean  $p\text{CO}_2$ , and seasonal biological and temperature effects, *Deep-Sea Res. Pt. II*, 49, 1601–1622, 2002.
- Takahashi, T., Sutherland, S., Wanninkhof, W., Sweeney, C., Feely, R. A., Chipman, D. W., Hales, B., Friederich, G., Chavez, F., Sabine, C., Watson, A., Bakker, D. C. E., Schuster, U., Metzl, N., Yoshikawa-Inoue, H., Ishii, M., Midorikawa, T., Nojiri, Y., Körtzinger, A., Steinhoff, T., Hoppema, M., Ólafsson, J., Arnarson, T. S., Tilbrook, B., Johannessen, T., Olsen, A., Bellerby, R., Wong, C. S., Delille, B., Bates, N. R., and de Baar, H. J. W.: Climatological mean and decadal change in surface ocean  $p\text{CO}_2$ , and net sea-air  $\text{CO}_2$  flux over the global oceans, *Deep-Sea Res. Pt. II*, 56, 554–577, doi:10.1016/j.dsr2.2008.12.009, 2009.
- Tanhua, T., Steinfeldt, R., Key, R. M., Brown, P., Gruber, N., Wanninkhof, R., Perez, F., Körtzinger, A., Velo, A., Schuster, U., van Heuven, S., Bullister, J. L., Stendardo, I., Hoppema, M., Olsen, A., Kozyr, A., Pierrot, D., Schirnack, C., and Wallace, D. W. R.: Atlantic Ocean CARINA data: overview and salinity adjustments, *Earth Syst. Sci. Data*, 2, 17–34, doi:10.5194/essd-2-17-2010, 2010.
- Taylor, K. E.: Summarizing multiple aspects of model performance in a single diagram, *J. Geophys. Res.*, 106, 7183–7192, 2001.
- Thomas, H., Friederike Prowe, A. E., Lima, I. D., Doney, S. C., Wanninkhof, R., Greatbatch, R. J., Schuster, U., and Corbière, Changes in the North Atlantic Oscillation influence  $\text{CO}_2$  uptake in the North Atlantic over the past 2 decades, *Global Biogeochem. Cy.*, 22, GB4027, doi:10.1029/2007GB003167, 2008.
- Tjiputra, J. F. and Winguth, A. M. E.: Sensitivity of sea-to-air  $\text{CO}_2$  flux to ecosystem parameters from an adjoint model, *Biogeosciences*, 5, 615–630, doi:10.5194/bg-5-615-2008, 2008.
- Tjiputra, J. F., Polzin, D., and Winguth, A. M. E.: Assimilation

- of seasonal chlorophyll and nutrient data into an adjoint three-dimensional ocean carbon cycle model: Sensitivity analysis and ecosystem parameter optimization, *Global Biogeochem. Cy.*, 21, GB1001, doi:10.1029/2006GB002745, 2007.
- Tjiputra, J. F., Assmann, K., Bentsen, M., Bethke, I., Otterå, O. H., Sturm, C., and Heinze, C.: Bergen Earth system model (BCM-C): model description and regional climate-carbon cycle feedbacks assessment, *Geosci. Model Dev.*, 3, 123–141, doi:10.5194/gmd-3-123-2010, 2010a.
- Tjiputra, J. F., Assmann, K., and Heinze, C.: Anthropogenic carbon dynamics in the changing ocean, *Ocean Sci.*, 6, 605–614, doi:10.5194/os-6-605-2010, 2010b.
- Ullman, D. J., McKinley, G. A., Bennington, V., and Dutkiewicz, S.: Trends in the North Atlantic carbon sink: 1992–2006, *Global Biogeochem. Cy.*, 23, GB4011, doi:10.1029/2008GB003383, 2009.
- Velo, A., Perez, F. F., Brown, P., Tanhua, T., Schuster, U., and Key, R. M.: CARINA alkalinity data in the Atlantic Ocean, *Earth Syst. Sci. Data*, 1, 45–61, doi:10.5194/essd-1-45-2009, 2009.
- Visbeck, M., Chassignet, E. P., Curry, R. G., Delworth, T. L., Dickson, R. R., and Krahnemann, G.: The ocean's response to North Atlantic Oscillation variability, in: *The North Atlantic Oscillation, Climate Significance and Environmental Impact*, edited by: Hurrell, J. W., Kushnir, Y., Ottersen, G., Visbeck, M., AGU Geophysical Monograph, 134, American Geophysical Union, Washington, DC, 113–146, 2003.
- von Storch, H. and Zwiers, F. W.: *Statistical Analysis in Climate Research*, Pergamon, Oxford, UK, 442 pp., 2002.
- Wanninkhof, R.: Relationship between wind speed and gas exchange over the ocean, *J. Geophys. Res.*, 97, 7373–7382, 1992.
- Wanninkhof, R., Olsen, A., and Triñanes, J.: Air-sea  $\text{CO}_2$  fluxes in the Caribbean Sea from 2002–2004, *J. Mar. Sys.*, 66, 272–284, doi:10.1016/j.jmarsys.2005.11.014, 2007.
- Watanabe, M. and Kimoto, M.: On the persistence of decadal SST anomalies in the North Atlantic, *J. Climate*, 13, 3017–3028, 2000.
- Watson, A. J., Schuster, U., Bakker, D. C. E., Bates, N. R., Corbière, A., González-Dávila, M., Friedrich, T., Hauck, J., Heinze, C., Johannessen, T., Körtzinger, A., Metzl, N., Olafsson, J., Olsen, A., Oschlies, A., Padin, X. A., Pfeil, B., Santana-Casiano, J. M., Steinhoff, T., Telszewski, M., Rios, A. F., Wallace, D. W. R., and Wanninkhof, R.: Tracking the variable North Atlantic sink for atmospheric  $\text{CO}_2$ , *Science*, 326, 1391–1393, 2009.
- Weiss, R. F.: Carbon dioxide in water and seawater: the solubility of a non-ideal gas, *Mar. Chem.*, 2, 203–215, 1974.
- Weiss, R. F.: Determination of carbon dioxide and methane by dual catalyst flame ionization chromatography and nitrous oxide by electron capture chromatography, *J. Chromatogr. Sci.*, 19, 611–616, 1981.
- Zeebe, R. E. and Wolf-Gladrow, D. E.:  *$\text{CO}_2$  in Seawater: Equilibrium, Kinetics, Isotopes*, Elsevier Oceanography Series, vol. 65, Elsevier, Amsterdam, The Netherlands, 346 pp., 2001.